Reverse Power Flow Detection Using Optimally Placed μPMUs in a Distribution System

Philip Joshua P. Eloja, Niko Avel F. Jorda, and Michael Angelo A. Pedrasa(✉)

Electrical and Electronics Engineering Institute, University of the Philippines Diliman, 1101 Quezon City, Philippines
philip.eloja@eee.upd.edu.ph, {nfjorda,mapedrasa}@up.edu.ph

Abstract. The rise in the accessibility of photovoltaic (PV) generators to consumers increases the possibility of reverse power flow (RPF) in the electric distribution system. RPF occurs when power flows to the design of the system. Overvoltage, power losses and protection system coordination are among the problems that could occur due to the presence of RPF. This paper describes an algorithm to detect the presence of RPF using optimally-placed micro-phasor measurement units (μPMUs) in the IEEE 34-Bus System with 5 PV generators. A machine learning algorithm based on a feedforward artificial neural network (ANN) was developed. The algorithm was able to detect the presence of RPF using (1) voltage and current and (2) polar- and (3) rectangular-impedance methods for training. The algorithm was also able to detect RPF under scenarios that were not used during the training process. Sensitivity analyses were performed for cases such as PV outage, PV relocation, PV addition, PV expansion and load increase. The susceptibility of the algorithm to true value errors (TVEs) was tested by adding error vectors on the μPMU measurements for both the training and testing populations.

Keywords: Reverse power flow (RPF) · μPMU · Machine learning

1 Introduction

Photovoltaic (PV) generators have been a great addition to the electric power system (EPS) in terms of its supply of sustainable energy. The sun is a renewable energy source that can be placed anywhere in the power system. As a solar farm, it can deliver bulk amounts of power to the grid. As an additional source of power for commercial and residential units, it can lower monthly electricity bills and export power to the network when it produces excess energy.

But with PV generators installed more and more in distribution systems as price drops, reverse power flow (RPF) becomes a problem. RPF occurs when power flows opposite where the system designed for it to flow which could be a huge risk for the distribution network as most of these systems are only designed to absorb power and not deliver power. Problems associated with RPF include, overvoltage, distribution protection coordination and power quality. [1] has claimed that RPF is the major cause of overvoltage in the distribution system. [2] has suggested that DGs could change short

J. L. Afonso et al. (Eds.): SESC 2019, LNICST 315, pp. 98–109, 2020.
https://doi.org/10.1007/978-3-030-45694-8_8

circuit levels in the system compromising the coordination of protection devices. According to [3], DGs may increase the power loss of the system depending on its network configuration.

2 Related Works

2.1 Micro-Phasor Measurement Unit (μPMU)

Growth in DGs in distribution network presents variability and uncertainty. As such, a more fast and precise measurement device needs to be developed to accurately assess the state of the system. The researchers in [4] addressed the issues faced by traditional supervisory control and data acquisition monitoring systems by developing a phasor measurement unit (PMU) that provides real-time and synchronized measurements. PMUs are more commonly used in transmission systems. In [5], the researchers further improved PMUs into micro-synchrophasors which can be used even in distribution systems. A micro-phasor measurement unit (μPMU) is a high-precision measurement unit that uses synchrophasor technology to observe the state of electric power systems. It can estimate the magnitude and phase angle of voltages and currents in the distribution system.

Optimal μPMU Placement (OPP) Problem. Installing μPMU in each node of the system would be ideal but not economical. But with the assumption that line data are available an optimal number of μPMU can be used to observe the system while reducing the cost. The fitness function that represents the OPP problem for an n-bus system is: [6]

$$\sum_{i}^{n} w_i x_i \tag{1}$$

where w_i is the cost and x_i is the binary decision variable of installing a PMU at bus i. A significant number of studies [6–9] have solved the OPP problem in various bus systems using different optimization algorithms.

2.2 Reverse Power Flow Detection

Directional relays have been in used to detect RPF in synchronous generators [10]. In [11] a directional power relay was employed to protect a distribution system from RPF caused by DG. The directional relays, however, are generally used to automate trippings due to faults.

[12] used an electronics-based transformer called a smart transformer to control the reverse power flows in the system. While this is a novel solution, the production of power can be more economical when the energy source is generous thus limiting its production is not the best option. With a proper analysis tool using the reverse power flow to the advantage of the system could be better by diverting where power is needed. But in order for such a tool to be used, an analysis to determine whether RPF is present in the system or not is needed.

Voltage Angle Difference Method. Consider two adjacent buses bus j and k. It can be seen in Eq. 2 that the sign of P_k and therefore its direction is related by the value of the angle inside the sine function. When θ_j is greater than θ_k the quantity inside the sine function is negative making the value of P_k negative since sine is an odd function. For the Reactive power on the other hand the direction of power of Q_k is dictated by V_k and V_j. When V_j is greater than V_k, the reactive power is negative.

$$P_k = \frac{|V_k||V_j|}{X}\sin(\theta_k - \theta_j) \tag{2}$$

$$Q_k = \frac{|V_k|}{X}\left[|V_k| - |V_j|\cos(\theta_k - \theta_j)\right] \tag{3}$$

$P_{k:}$ real power injection through bus k
Q_k: reactive power injection through bus k
V_k: voltage magnitude at bus k
$V_{j:}$ voltage magnitude at bus j
$\theta_{k:}$ voltage angle at bus k
$\theta_{j:}$ voltage angle at bus j
X: line impedance from bus k to j

In this paper, only the fundamental frequency was considered due to the high sampling rate of μPMUs.

Impedance Method. A relationship between power and impedance can also be drawn, [1] uses this method to determine at what impedance level the reverse power flow occurs from PV injections. Impedance as seen by bus k can be expressed as:

$$Z_k = \frac{V_k}{I_k} \tag{4}$$

$$Z_k = \frac{V_k}{\left(\frac{P_k + Q_k}{V_k}\right)^*} \tag{5}$$

$$Z_k = \left(\frac{P_k + jQ_k}{P_k^2 + Q_k^2}\right)|V_k|^2 \tag{6}$$

I_k: current going through bus k to bus j

Equation 6 can be further decomposed to its resistance (R_k) and reactance (X_k) components.

$$R_k = \left(\frac{P_k}{P_k^2 + Q_k^2}\right)|V_k|^2 \tag{7}$$

$$X_k = \left(\frac{Q_k}{P_k^2 + Q_k^2}\right)|V_k|^2 \tag{8}$$

As P_k flows to the opposite direction, the value of R_k and X_k will be negative.

2.3 Classification Algorithms in Machine Learning

There are several techniques in tackling classification problems such as support vector machines (SVM), random tree and neural networks among others. For the purposes of this study, the proponents will be focusing on neural networks.

Neural Networks. Neural Network or also known as artificial neural networks (ANN) is a problem-solving technique developed to tackle non-linear and complex problems [13]. For [14], ANN is one of the best techniques for data classification.

Primarily, the ANN is composed of two major components, the neurons and connections [15]. To put it simply, neurons are the data processing units of the algorithm. It analyzes inputs and its relation to the output in order to create a relationship between the two. Connections, on the other hand, are the one that delivers this data from neuron to neuron. It is the carrier of information.

While there are a number of topologies in the ANN architecture, the most popular is the feedforward network [15] shown in Fig. 1. This topology consists of three or more layers. The first layer is called the input layer, the next layers are called the hidden layer, while the last layer is called the output layer. In this setup, data travels from one layer to another without reversing. The bulk of the processing happens in the hidden layer.

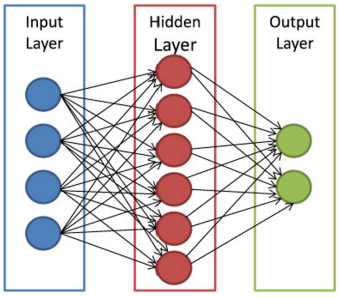

Fig. 1. Feedforward topology

3 Methodology

3.1 Testbed Creation

To develop an algorithm that can detect the presence of RPF, a testbed is needed in order to train and test it. This testbed was created using OpenDSS.

Bus System Modelling. The proponents adapted the bus network used in [10] as shown in the Fig. 2 while modifying the placement of μPMU in node 836 to node 860. μPMU will be placed on primary lines just before buses 814, 852 and 860 to measure voltages and currents of the lines and not the buses itself. A μPMU is also placed just after reference bus 800. The system will have 5 3-phase PVs attached to buses, 808, 824, 830, 844 and 860. Capacities of these PVs can be seen in Table 1.

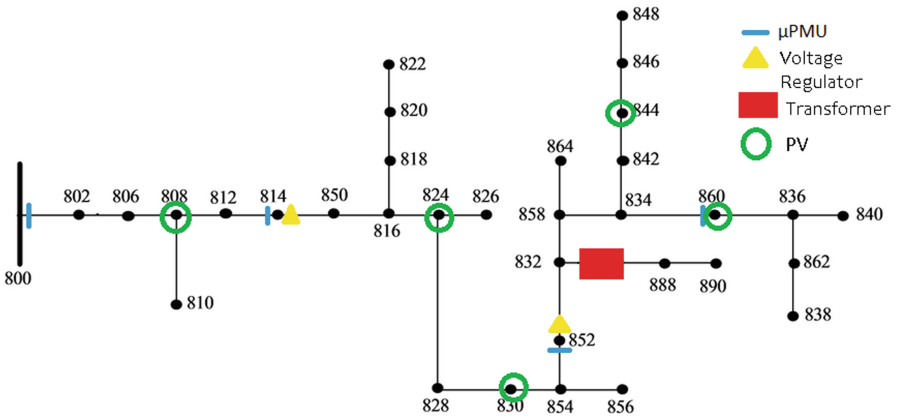

Fig. 2. Modified IEEE-34 bus network with optimally placed μPMUs

Table 1. 3-phase PV locations and capacities

PV location	PV capacity per phase (kW)
Bus 808	180
Bus 824	100
Bus 830	200
Bus 860	100
Bus 844	140

Bus System Modeling. There were 3 different types of samples that were generated: (1) average loading, (2) variable loading and (3) PV outage with variable loading.

For the first type of samples shown in Fig. 3, the percent loading of each bus will be varied from each other while maintaining a mean percent loading for the whole system. The mean percent loading will be swept from 20% to 100% with a 2% increment. With this, percent loading for each bus will deviate by around 5% from the suggested mean percent loading across the system. For each increment of the mean percent loading, the 5 PVs will be injecting real power to the system from 0% capacity to 100% capacity incremented uniformly by 1%. 4100 samples will be generated from this method.

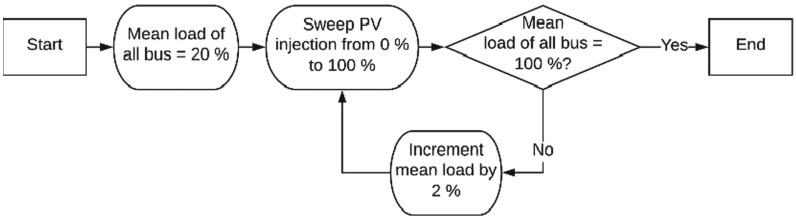

Fig. 3. Process of generating the samples with average loading

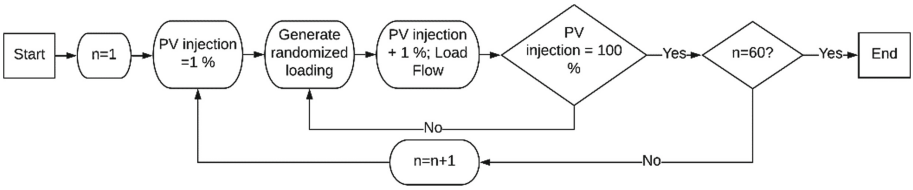

Fig. 4. Process of generating the sample with variable loading

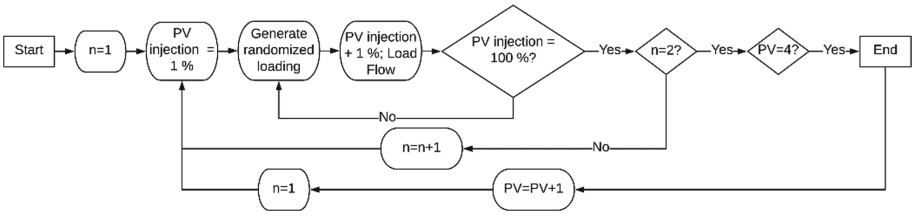

Fig. 5. Process of generating the samples for PV outage with variable loading

For the second type of samples, as shown in Fig. 4, percent loading for each bus in the system will be varied from each other. This method will ensure that as the 5 PVs injects power from 0% to 100%, each 1% increment of power injection will have a different set of percent loading for each bus that will be varied from 20% to 100%. This method will generate a batch of samples that will be as varied from each other as possible. 6000 samples will be generated from this method.

For the third type of samples shown in Fig. 5, PV Outage will be simulated. Percent loading of each bus will be acquired using the method for acquiring percent loading in the second type of samples. PVs in operation will be decreased from 5 PVs up to 1 PV while considering all 30 possible combinations for PV operation. For each combination 200 samples were generated which amounted to 6000 samples.

Each sample generated have a tag of 0 if RPF is not present in the system and 1 if RPF is present. Impedance method was used to tag each sample. Since RPF will first occur on buses where generators are present, impedances as seen on the buses where PVs are placed were computed. Where resistance was seen as negative in a bus, there is RPF in the system.

Introduction of TVEs in the Training Population. Data from μPMU will deviate from the true values of currents and voltages in the system by 0.1%. The proponents added True Value Errors (TVEs) to the previously generated samples to make another set of training population. Equation 9 shows how the errors were introduced to the original voltage and current measurements gathered from the 4 μPMUs.

$$A^* = A + \left[e(|A|\angle\delta)\right] \tag{9}$$

Where,

A: phasor measurement
A*: phasor measurement with TVE
E: random value from −0.001 to 0.001
Δ: random angle value from 0^o to 360^o

3.2 Machine Learning Implementation

Algorithm Training and Testing. Three models for the RPF detection were used. One model had 48 inputs which consists of 12 voltage magnitudes, 12 current magnitude and 18 phasor angles. The second model used the impedances calculated, in polar form, from μPMU measurements of which there will be 24 inputs - 12 magnitude measurements and 12 angles measurements. The third model was derived from the polar form of the impedance by converting it to its rectangular form. There will be 24 inputs from this method with 12 resistance and 12 reactance. For all model there will only be two outputs, 1 which denotes the presence of RPF within the system and 0 which denotes otherwise. The MATLAB's Deep Learning Toolbox was used in training the algorithm with a feedforward topology and 10 hidden nodes in the ANN architecture. 80% of the 16,100 samples were used for the training of the algorithm while the remaining 20% were used for testing.

Performance Evaluation. The algorithms developed were subjected to another round of testing using 1000 samples that were generated outside of the 16100 samples of the training population. The results of the testing using these samples will serve as the base case.

Sensitivity Analysis. The trained algorithms were tested using test samples that were not included in the training population. Five scenarios were established to test the robustness of the algorithm. For each case 1000 test samples were generated.

PV Outage. The system simulated events wherein 1 or more PVs are offline. The number of functioning PVs was reduced decrementally from 5 to 1. PVs were relocated to the adjacent 3-phase bus one at a time. Each of the 5 PVs, while retaining their capacity output, were relocated twice, as there were two adjacent buses for each of the PVs.

PV Relocation. The PVs were relocated to their adjacent 3-phase bus one at a time. Each of the 5 PVs were relocated twice, as there were two adjacent buses for each of the PVs. The capacities of the PVS were retained.

PV Addition. Another 3-phase PV Generator was added to a random bus in the IEEE-34 bus system, making the total number of PVs to 6. The addition of 3-phase PV to the system will be repeated 10 times amounting to 1000 test samples (Table 2).

Table 2. Sizing and placement of additional PV

Bus	Capacity per phase (kW)	Voltage (kV)
840	10	14.376
890	70	2.401
848	20	14.376
858	80	14.376
816	50	14.376
802	100	14.376
854	50	14.376
850	75	14.376
832	80	14.376
828	75	14.376

PV Expansion. The capacities of the 5 existing 3-phase PVs were increased while maintaining the per-unit voltage of the system to 1.1 p.u. A total of 100 kW was added to the total PV power output (Table 3).

Table 3. New PV capacity after expansion

PV location	New PV capacity per phase (kW)
Bus 808	180
Bus 824	100
Bus 830	200
Bus 860	100
Bus 844	140

Load Increase. An increase in power consumption was simulated for this test case. The base loads of each bus were increased to up to 150% while still retaining the old capacities of the 5 PVs.

Introduction of TVEs in the Testing Population. TVEs were also introduced to the 5000 test samples generated for the sensitivity analysis. This will test the susceptibility of the algorithms trained to errors in the measurements. All of the testing mentioned above were repeated after adding TVEs.

4 Results and Analysis

Algorithms developed have significantly high accuracies and are close to each other whether trained using the standard training population set or the modified training population with accuracies up to 99.7%. Upon evaluating the performance of the algorithms, the accuracies scored near the 99% mark (Tables 4 and 5).

Table 4. Accuracy results of the algorithm training and testing

Algorithm method	Algorithm accuracy with standard training population	Algorithm accuracy with modified training population
Voltage and current	99.7	99.7
Polar impedance	98.7	98.9
Rectangular impedance	98.5	98.6

Table 5. Accuracy results of the algorithm performance evaluation

Algorithm method	Algorithm accuracy with standard training population	Algorithm accuracy with modified training population
Voltage and current	98.7	98.8
Polar impedance	99.2	98.9
Rectangular impedance	98.2	98.3

For the sensitivity analysis of the algorithms developed using the standard training population using test samples with no TVE, accuracies are above 90%. PV outage, PV relocation and PV expansion are the only scenarios where the algorithm only got almost 93% as the rest scored above 95%. Upon the introduction of TVE in test samples however, for the voltage and current method, accuracies are down to almost 50%. Both the algorithms using impedance method scored the same accuracies as their counterpart algorithm (Tables 6 and 7).

Table 6. Accuracy results for the sensitivity analysis of algorithms for standard training population without TVE

Test case	Voltage and current method	Polar impedance method	Rectangular impedance method
Base case	98.7	99.2	98.2
PV outage	93.9	93.6	93.3
PV relocation	93.6	93.1	92.4
PV addition	98.5	98.8	98
PV expansion	98.6	99.1	98.5
Load increase	92.8	95.4	92.5

Table 7. Accuracy results for the sensitivity analysis of algorithms for standard training population with TVE

Test case	Voltage and current method	Polar impedance method	Rectangular impedance method
Base case	53.4	99.2	98.2
PV outage	52.3	93.6	93.3
PV relocation	52.6	93.1	92.4
PV addition	53.6	98.9	98
PV expansion	53.7	99.1	98.5
Load increase	54	95.4	92.5

The algorithms with a modified training population on the other hand had high accuracy results for the sensitivity analysis. The voltage and current method had also significantly improved accuracies for all test cases where test samples have been introduced with TVE (Tables 8 and 9).

Table 8. Accuracy results for the sensitivity analysis of algorithms for modified training population without TVE

Test case	Voltage and current method	Polar impedance method	Rectangular impedance method
Base case	98.8	98.9	98.3
PV outage	93.8	93.8	94.4
PV relocation	93.1	93.5	92.4
PV addition	98.7	98.7	97.6
PV expansion	98.7	98.7	98.8
Load increase	96.8	93.4	97.8

Table 9. Accuracy results for the sensitivity analysis of algorithms for modified training population with TVE

Test case	Voltage and current method	Polar impedance method	Rectangular impedance method
Base case	98.6	98.9	98.4
PV outage	94.1	93.8	94.3
PV relocation	93	93.6	92.4
PV addition	98.8	98.7	97.6
PV expansion	98.7	98.7	98.8
Load increase	97.4	93.4	97.8

5 Conclusion

This paper describes machine learning algorithms based on ANN that can detect reverse power flow in distribution networks with PV generators. The algorithm uses measurements gathered by optimally placed μPMU along the network and another μPMU in the substation bus. Several algorithms were developed: one using the raw phasor voltage and current measurements as inputs and two using the apparent downstream impedance as inputs (first has the impedance in rectangular form, and other in polar form).

The IEEE 34-bus system with 5 PV generators and 3 optimally placed μPMUs was used to demonstrate the performance of the system. The robustness of the algorithm was also investigated by adding noise to the measurements and using the algorithm to detect RPF on a network that is slightly different from the network where training data was gathered. The algorithms were able to detect RPF with high accuracy except on cases where the testing data contained measurement errors while the training population did not. The performance improved when the algorithm was trained using measurements that contained noise.

References

1. Mortazavi, H., Mehrjerdi, H., Saad, M., Lefebvre, S., Asber, D., Lenoir, L.: A monitoring technique for reversed power flow detection with high PV penetration level. IEEE Trans. Smart Grid **6**, 2221–2232 (2015)
2. Antonova, G., Nardi, M., Scott, A., Pesin, M.: Distributed generation and its impact on power grids and microgrids protection. In: 2012 65th Annual Conference for Protective Relay Engineers, pp. 152–161 (2012)
3. Sarabia, A.: Impact of distributed generation on distribution system. Master's thesis, Department of Energy Technology Aalborg University, Pontoppidanstraede 101, 9220 Aalborg East Denmark (2011)
4. Phadke, A.G., Thorp, J.S., Karimi, K.J.: State estimlatjon with phasor measurements. IEEE Trans. Power Syst. **1**, 233–238 (1986)
5. von Meier, A., Culler, D., McEachern, A., Arghandeh, R.: Micro-synchrophasors for distribution systems. In: ISGT 2014, pp. 1–5 (2014)
6. Mabaning, A.A.G., Orillaza, J.R.C., von Meier, A.: Optimal PMU placement for distribution networks. In: 2017 IEEE Innovative Smart Grid Technologies - Asia (ISGT-Asia), pp. 1–6 (2017)
7. Tahabilder, A., Ghosh, P.K., Chatterjee, S., Rahman, N.: Distribution system monitoring by using micro-PMU in graph-theoretic way. In: 2017 4th International Conference on Advances in Electrical Engineering (ICAEE), pp. 159–163 (2017)
8. Al Rammal, Z., Abou Daher, N., Kanaan, H., Mougharbel, I., Saad, M.: Optimal PMU placement for reverse power flow detection, pp. 1–5 (2018)
9. Jamei, M., et al.: Anomaly detection using optimally placed μPMU sensors in distribution grids. IEEE Trans. Power Syst. **33**, 3611–3623 (2018)
10. Yaghobi, H.: Fast predictive technique for reverse power detection in synchronous generator. IET Electr. Power Appl. **12**(4), 508–517 (2018)
11. Sudhakar, P., Malaji, S., Sarvesh, B.: Reducing the impact of dg on distribution networks protection with reverse power relay. In: International Conference on Processing of Materials, Minerals and Energy. Materials Today: Proceedings, Ongole, Andhra Pradesh, India, 29th–30th July, vol. 5, no. 1, Part 1, pp. 51– 57 (2016)

12. De Carne, G., Buticchi, G., Zou, Z., Liserre, M.: Reverse power flow control in a st-fed distribution grid. IEEE Trans. Smart Grid **9**, 3811–3819 (2018)
13. Lari, N.S., Abadeh, M.S.: Training artificial neural network by krill-herd algorithm. In: 2014 IEEE 7th Joint International Information Technology and Artificial Intelligence Conference, pp. 63–67 (2014)
14. Hong, Z.: A preliminary study on artificial neural network. In: 2011 6th IEEE Joint International Information Technology and Artificial Intelligence Conference, vol. 2, pp. 336–338 (2011)
15. Kriesel, D.: A brief introduction to neural networks (2007)